FEBRUARY 15, 1930 PHYSICAL REVIEW VOLUME 35

FINE STRUCTURE OF THE BERYLLIUM FLUORIDE BANDS

By F. A. Jenkins
Department of Physics, University of California

(Received December 24, 1929)

Abstract

Wave-length measurements of BeF bands.—New wave-length measurements have been made of the rotational lines of the BeF bands in the regions λλ3009.5–3026.3, 2908.9–2927.8, and 3126.1–3140.8, which include all the stronger lines of the (0, 0), (1, 0) and (0, 1) bands. The source was a cored carbon arc run at atmospheric pressure. The Harvard 21-foot grating was used in the second order, giving a linear dispersion of 0.97 A per mm and an effective resolving power of nearly 100,000. The wave-numbers of the lines in the six branches of each band are tabulated for rotational quantum numbers up to about $K=50$ in the R branches, 45 in the Q branches, and 30 in the P branches. Visual intensity estimates are also included.

Term analysis of BeF bands.—The rotational structure is found to be that characteristic of a $^2\Pi \rightarrow {}^2\Sigma$ electronic transition, with a relatively small value of $\Delta E/B$, $+15.667$, in the Π state. The combination relations among the lines of the (1, 0), (0, 0) and (0, 1) bands are satisfied within the experimental error in every case where exact agreement is to be expected. The R-Q, Q-P relations show a small combination defect, which is referred to Λ-type doubling in the initial state. This doubling is slightly greater for the levels involved in the low-frequency sub-band, and therefore it is assumed that the $^2\Pi$ state is normal. Rotational terms having the same K in the initial state draw rapidly together as the rotation increases, due to the loose coupling of the spin with the molecular axis. Quantitative agreement is obtained between the observed term-differences, ΔF, and their values calculated by the theoretical energy formulas derived by Hill and Van Vleck for the transition from case a to case b type of spin coupling. Equations capable of representing all the lines in a given band are deduced.

Constants of BeF molecule.—The following values for the more important molecular constants are obtained: $B^{(0)\prime}=1.41060$ cm^{-1}, $B^{(0)\prime\prime}=1.47928$, $\alpha'=0.01610$ cm^{-1}, $\alpha''=0.01685$, $D^{(0)\prime}=-8.301\times10^{-6}$ cm^{-1}, $D^{(0)\prime\prime}=-8.209\times10^{-6}$, $\beta'=1.060\times10^{-8}$ cm^{-1}, $\beta''=2.903\times10^{-8}$, $I_e'=(19.50\pm0.03)10^{-40}$ g cm^2, $I_e''=(18.59\pm0.03)10^{-40}$, $r_e'=1.390\times10^{-8}$ cm, $r_e''=1.357\times10^{-8}$, $\omega_e'=1172.56$ cm^{-1}, $\omega_e''=1265.62$, $x_e'=0.007488$, $x_e''=0.007206$, $\nu_e=33{,}233.61$ cm^{-1}, $\Delta E=22.10\pm0.1$ cm^{-1}.

Introduction

BAND spectra are known for a large number of diatomic alkaline earth halides,[1] the most familiar being those of the fluorides, such as CaF. In general, the rotational structure of these bands is so finely spaced that there seems to be little hope of carrying out a detailed fine structure analysis, even

---

[1] For the experimental material on the alkaline earth halides, other than BeF, see H. Kayser, "Handbuch der Spectroscopie," Vols. 5, and 6, and S. Datta, Proc. Roy. Soc. **99A** 436 (1921). General treatments of the relations between the electronic states, molecular constants, etc., have been given by R. Mecke, Zeits. f. Physik **42**, 390 (1927) and by R. C. Johnson, Proc. Roy. Soc. **122A**, 161, 189 (1929).

with spectrographs of the highest resolving power. The most favorable case for analysis is the lightest molecule of this class, BeF, for which, owing to its small moment of inertia, the spacing of the lines in a band should be great enough to permit almost complete resolution. A band system due to this molecule was first reported by Datta[2] in 1922. Its bands are shaded toward the red and lie completely in the ultra-violet, the head of the strongest occurring at λ3009.6. Datta undertook a study of the fine structure of this band, and was able to identify three fairly regular series of lines. It is obvious, however, from an examination of his reproduction, and of the curves obtained, that the resolving power he used (third order of a 10-foot grating) was insufficient for a satisfactory quantum analysis of the band structure. Each of his series, as will appear in the present work, represents the blending of two or more true series. For the analysis to be reported here, new plates were taken, having a dispersion and actual resolution from 2 to 3 times greater than those attained by Datta. This comparatively small advantage has made possible a complete and satisfactory interpretation of the rotational structure.

The BeF bands were first considered from the standpoint of the quantum theory by Mulliken.[3] Vibrational quantum numbers were assigned, and an equation derived for the frequencies of the heads, as measured by Datta. The molecule BeF was classed with a number of one-valence-electron emitters of band spectra, such as BO, CN, CO^+, N_2^+, the spectra of which appeared to be qualitatively similar. From such considerations, it was concluded that the ultra-violet BeF system represents a $^2\Pi \rightarrow {}^2\Sigma$ electron jump, analogous to the α bands of BO, the red CN bands, etc. The latter are of the double double-headed type, the first head in each pair being formed by an R, and the second by a Q branch.[4] Each of the BeF bands has only 3 heads, the first two forming a close pair of nearly equal intensity, and the third being somewhat weaker. It has therefore been assumed that the second and third heads are those of the Q branches, the second R head being too faint to be observed. On this view, the two Q heads should represent approximately the double origin of the band and from these $\Delta E \leqq 35$ cm^{-1} for the $^2\Pi$ state. A revised interpretation of the formation of the heads has recently been given by Jevons.[5] From a critical study of Datta's measurements, especially with regard to the variation of the mutual separations of the heads with vibrational quantum number, he concluded that the first pair of heads is formed by two closely parallel R branches and the third by one of two Q branches. Evidence for a second Q head was found on the writer's spectrograms early in the present work, but it appeared later during the analysis that this apparent head is merely a fortuitous accumulation of lines at the point in question.

In beginning the analysis of a band of complex structure, it is very desirable to have as a starting point an approximate idea of the type of band

---

[2] S. Datta, Proc. Roy. Soc. **101A,** 187 (1922). An excellent reproduction of the band system as a whole is given.

[3] R. S. Mulliken, Phys. Rev. **26,** 561 (1925).

[4] F. A. Jenkins, Proc. Nat. Acad. **13,** 496 (1927).

[5] W. Jevons, Proc. Roy. Soc. **122A,** 216 (1929).

structure, i.e. number of branches, approximate electronic separation, etc. According to the revised interpretation by Jevons, the rotational structure of the BeF bands should resemble that of the green MgH bands, where the electronic doublet separation is relatively small, and the corresponding branches of the two sub-bands draw rapidly together with increasing rotational quantum number. Bands showing this type of "rotational distortion" are fairly numerous[6] and, as in BeF, three heads are usually observed, one of the Q branches not forming a head due to the distortion effect. Such a structure is characteristic of a $^2\Pi\rightarrow{}^2\Sigma$ or $^2\Sigma\rightarrow{}^2\Pi$ transition, in which the ratio of the doublet energy difference, ΔE, to the constant B, is small (i.e. less than about 20). A point strongly opposed to the previous interpretation, with $\Delta E/B$ large, appeared in the fact that, although the bands are closely grouped in sequences the distance from the R head to the origin would be extremely small (3 cm^{-1}). This would violate the rule of Birge and Mecke, according to which a small change in the vibration frequency during the transition is always accompanied by a small change in the moment of inertia. It therefore seemed probable that in BeF the $\Delta E/B$ is small. By postulating that the bands are of the MgH type, preliminary investigations of the structure[7] showed that Jevons' scheme is essentially correct.

EXPERIMENTAL PROCEDURE

The spectrograms were obtained in the second order of the 21-foot grating at Harvard University, giving a dispersion of 0.97A per mm in the region investigated. An arc in air between carbon poles, both cored with a mixture of $BeKF_3$ and powdered carbon, gives not only the BeF, but also the BeO band system with considerable intensity in the flame surrounding the poles.[8] Therefore, the BeO bands were also obtained on these plates. The rotational quantum analysis of the latter system has been given by Miss J. E. Rosenthal and the writer,[9] and also independently by Bengtsson.[10] In the former article will be found a brief description of the experimental details pertaining to the spectrograms used in the present investigation, since the BeF and BeO spectra were photographed simultaneously. Two sets of plates were of use for our purpose, one showing the stronger sequence $\Delta v=0$[11] with the best possible resolution (slow, fine-grained plates) and another on which the 0 sequence is considerably over-exposed, but the sequences +1 and −1 are of satisfactory

---

[6] R. S. Mulliken, Phys. Rev. **32**, 388 (1928).

[7] The main results embodied in the present article were given in a paper before the American Physical Society, Washington Meeting, April, 1929. Cf. Phys. Rev. **33**, 1090 (1929) (Abstract).

[8] Jevons, ref. 5, finds that the oxide bands are relatively stronger in the outer part of the flame.

[9] J. E. Rosenthal and F. A. Jenkins, Phys. Rev. **31**, 705 (Apr. 1928) (Abstract), Phys. Rev. **33**, 163 (1929).

[10] E. Bengtsson, Arkiv. för Mat. Astro. och Fysik, **20A**, No. 21, p. 1, June 1928.

[11] The nomenclature used here conforms with the revised system recently proposed (Mulliken, private communication). In this v represents the vibrational quantum number, formerly n.

intensity. The first heads of the three sequences are, according to Mulliken's assignment: λ3009.582 (0), λ2908.994 (−1) and λ3126.116 (+1). Doublets with a separation of 0.04A are resolved on these plates. The iron arc comparison spectrum shows no relative displacement on the two sets. An enlargement of part of the 0 sequence from the first set is shown in Fig. 1, accompanied by a Fortrat diagram of the (0, 0) band, according to our complete analysis.

In order to take full advantage of the combination principle, it was necessary to study bands which would yield agreements in the term-differences of both the initial and the final states. Accordingly, wave-length measurements were made of the lines in the first band of each of the three above-mentioned sequences, i.e. in the (0, 0), (1, 0) and (0, 1) bands. The secondary Fe wave-length standards given by Fabry[12] were used throughout. The measurements included every line in each sequence as far as the first head of the third band in that sequence. This was necessary because, as will be apparent in Fig. 1, many lines of the first band are intermingled with those of the second. In

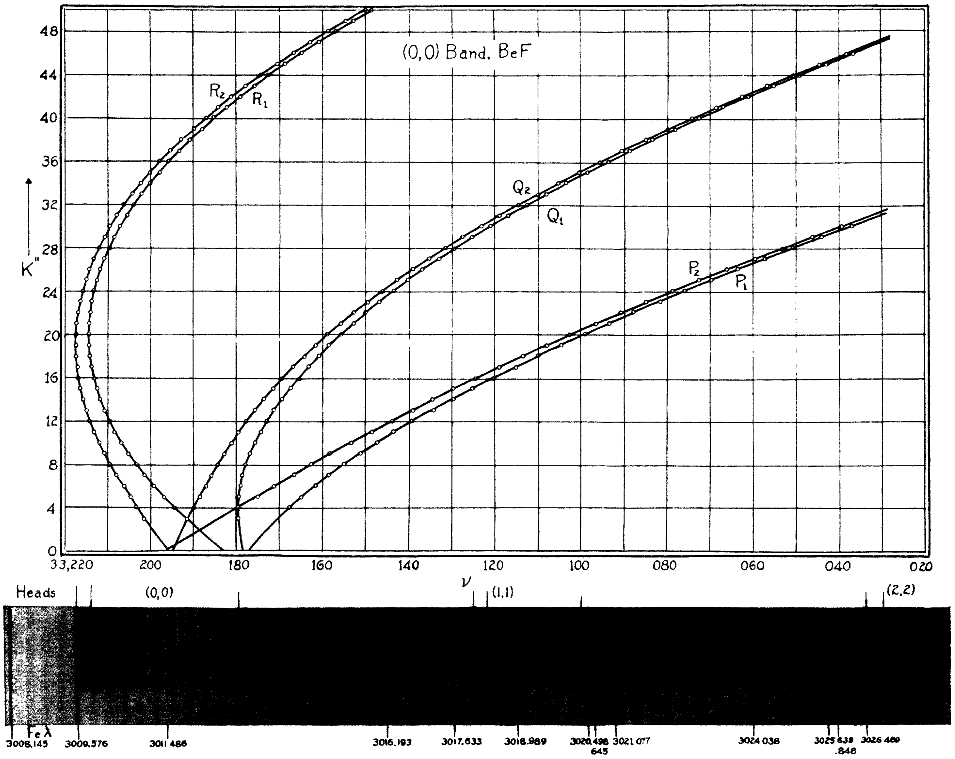

Fig. 1. (0, 0) *band of BeF.* The spectrum has been enlarged to practically the same scale as the diagram, but the correspondence of the lines with points on the diagram is not exact throughout, because the latter is on a scale of frequencies.

---

[12] Ch. Fabry, Int. Crit. Tables, Vol. V, p. 275.

general, our wave-lengths agree well with those of Datta.[2] Table I gives the wave-numbers in vacuum of all lines assigned to the above three bands. A large number of measured lines belonging to the second bands of the sequences are not given, because they represent only certain parts of these bands and would be of little value for the present purpose. Although there is an element

TABLE I. *Wave-number and intensity data for BeF bands.*

R$_2$ *head*, $\lambda_{air}=3009.582$			(0, 0) band *R*$_1$ *head*, $\lambda 3009.873$		*Q*$_1$ *head*, $\lambda 3013.011$	
K''	*R*$_2$	*R*$_1$	*Q*$_2$	*Q*$_1$	*P*$_2$	*P*$_1$
3	33,201.42^{2}1	33,191.43^{1}0	33,190.66^{2}3	—	—	—
4	203.21^{2}2	194.24^{1}1	189.85^{2}4	33,179.45^{3}4*d*	33,179.76^{2}2	33,167.42^{2}3*d*
5	205.06^{2}0	196.73^{1}1*d*	188.44^{1}1	179.45^{3}4*d*	174.92^{1}0	164.92^{2}3
6	206.71^{2}1	199.14^{1}1	187.03^{2}4	178.97^{2}1	171.26^{3}4	161.41^{3}4
7	207.84^{2}3	201.42^{2}1	185.74^{1}2	178.59^{1}1	166.59^{3}4	158.30^{2}5
8	209.47^{4}4*d*	203.21^{2}2	184.14^{2}4*d*	177.64^{3}5	161.41^{3}4	154.82^{1}1
9	210.71^{4}4	205.06^{2}0	182.74^{1}3	176.76^{1}2	156.87^{2}2	151.03^{1}2
10	211.77^{4}3*d*	206.71^{2}1	180.96^{2}4*d*	175.65^{3}5	153.18^{1}1	147.13^{1}0–
11	213.11^{4}3	208.38^{2}3	179.45^{3}4*d*	174.17^{2}3	148.42^{2}2*d*	143.36^{2}3*d*
12	214.18^{7}5*d*	209.47^{4}4*d*	177.64^{3}5	172.82^{1}2	143.89^{2}2	138.93^{4}4*d*
13	214.95^{2}2	210.71^{4}4	175.65^{3}5	171.26^{3}4	138.93^{4}4*d*	134.32^{3}3
14	215.69^{2}2	211.77^{4}3*d*	173.53^{1}2	169.30^{2}4*d*	134.32^{3}3	129.57^{3}3*d*
15	216.36^{2}1	212.44^{2}2	171.26^{3}4	167.42^{2}3*d*	129.57^{3}3*d*	125.00^{2}3
16	216.65^{1}1	213.11^{4}3	169.30^{2}4*d*	165.33^{1}3	124.22^{1}2	120.13^{1}1*d*
17	216.94^{2}1	213.75^{2}2	166.59^{3}4	163.08^{1}3	118.78^{2}4*d*	115.02^{2}2*d*
18	217.41^{4}5*d*	214.18^{7}5*d*	164.05^{1}3	160.77^{2}4	113.51^{1}2	109.75^{2}3
19	217.41^{4}5*d*	214.18^{7}5*d*	161.41^{3}4	158.30^{2}5	107.81^{2}4	104.48^{1}2
20	217.41^{4}5*d*	214.18^{7}5*d*	158.56^{2}5	155.58^{2}5	102.36^{1}2	099.04^{1}2
21	217.41^{4}5*d*	214.18^{7}5*d*	155.58^{2}5	152.59^{3}5	096.54^{1}3*d*	093.44^{2}3
22	216.94^{2}1	214.18^{7}5*d*	152.59^{3}5	149.87^{2}4*d*	090.71^{1}0*d*	087.67^{1}1*d*
23	216.36^{2}1	213.75^{2}2	149.28^{1}4	146.61^{1}3	084.82^{2}4	081.83^{1}2*d*
24	215.69^{2}2	213.11^{4}3	145.93^{1}3	143.36^{2}3*d*	078.58^{1}3*d*	075.89^{1}1
25	214.95^{2}2	212.44^{2}2	142.48^{1}4	139.96^{1}3	072.37^{2}4	069.49^{1}2*d*
26	214.18^{7}5*d*	211.77^{4}3*d*	138.93^{4}4*d*	136.47^{1}3	065.89^{1}3	063.30^{1}2*d*
27	213.11^{4}3	210.71^{4}4	135.10^{1}3	132.77^{1}3	059.46^{1}2	057.09^{1}3
28	211.77^{4}3*d*	209.47^{4}4*d*	131.19^{2}4	128.94^{1}5	052.86^{1}2	050.52^{2}5*d*
29	210.71^{4}4	208.38^{2}3	127.20^{1}3	125.00^{2}3	046.12^{1}4*d*	043.70^{1}2
30	209.47^{4}4*d*	207.02^{1}2	123.01^{1}4	120.82^{2}4	039.08^{1}4	036.84^{1}4
31	207.84^{2}3	205.44^{1}2	118.78^{2}4*d*	116.72^{1}2	—	—
32	205.98^{1}2	203.98^{2}3*d*	114.28^{1}3	112.38^{1}3*d*		
33	203.98^{2}3*d*	202.14^{2}4	109.75^{2}3	107.81^{2}4		
34	202.14^{2}4	200.03^{2}5	105.07^{1}3	103.14^{1}3		
35	200.03^{2}5	197.79^{2}4*d*	100.22^{1}3	098.30^{1}3*d*		
36	197.79^{2}4*d*	195.66^{1}4	095.27^{1}3*d*	093.44^{2}3		
37	195.27^{1}4	193.23^{1}3	090.20^{1}2*d*	088.41^{1}2*d*		
38	192.58^{1}3	190.66^{1}3	084.82^{2}4	083.17^{1}2		
39	189.85^{2}4	187.93^{1}3	079.49^{1}3	077.82^{1}3		
40	187.03^{2}4	185.10^{1}3	073.91^{1}4	072.37^{2}4		
41	184.14^{2}4*d*	182.08^{1}3	068.20^{1}4	066.69^{1}3		
42	180.96^{2}4*d*	178.97^{2}1	062.44^{1}4	060.96^{1}3		
43	177.64^{3}5	175.65^{3}5	056.61^{1}4	054.98^{1}3		
44	174.17^{2}3	172.10^{1}2	050.52^{2}5*d*	048.97^{1}3		
45	170.39^{1}3	168.60^{1}2	044.20^{1}3*d*	042.72^{1}3*d*		
46	166.59^{3}4	164.92^{2}3	037.90^{1}2	036.43^{1}5		
47	162.74^{1}2	160.77^{2}4	—	—		
48	158.56^{2}5	156.87^{2}2				
49	154.50^{1}1	152.59^{3}5				
50	149.87^{2}4*d*	148.42^{2}2*d*				
51	145.58^{1}2	143.89^{2}2				
52	140.85^{1}2	138.93^{4}4*d*				
53	136.12^{1}1	134.32^{3}3				
54	131.19^{2}4	129.57^{3}3*d*				
55	125.94^{1}1	—				

TABLE I. (Continued)

			(0, 1) band)			
R_2 *head*, λ3126.116			R_1 *head*, λ3126.366		Q_1 *head*, λ3130.369	
K''	R_2	R_1	Q_2	Q_1	P_2	P_1
5			31,941.19^{1}1			
6			940.39^{2}4	——		
7	——	——	939.28^{2}4	31,932.20^{1}1		
8	31,963.42^{4}5*d*	31,957.34^{2}2*d*	938.24^{1}2*d*	931.45^{2}3*d*		
9	964.92^{3}3	959.12^{1}2	937.37^{1}3	930.95^{1}2*d*		
10	966.43^{3}3	961.64^{4}5*d*	935.89^{1}2	929.89^{2}3*d*		
11	967.96^{3}3	963.42^{4}5*d*	934.40^{1}3*d*	929.01^{1}2*d*	——	——
12	969.38^{3}3	964.92^{3}3	932.99^{1}3*d*	928.60^{2}5*d*	31,899.20^{1}1	31,894.22^{1}1
13	970.72^{3}3	966.43^{3}3	931.45^{2}3*d*	927.06^{1}2	894.72^{1}1	889.94^{2}4
14	971.81^{2}4*d*	967.96^{3}3	929.89^{2}3*d*	925.60^{1}1	890.60^{1}0	886.24^{2}2
15	972.78^{4}4	969.38^{3}3	928.60^{2}5*d*	924.48^{2}5*d*	886.24^{2}2	881.65^{2}0*d*
16	974.32^{3}3*d*	970.72^{3}3	926.47^{1}2	922.73^{2}5	881.65^{2}0*d*	877.37^{1}0
17	975.02^{4}4	971.43^{2}3*d*	924.48^{2}5*d*	921.14^{1}4	876.74^{2}2	873.22^{2}4
18	975.66^{4}4*d*	972.78^{4}4	922.73^{2}5	919.36^{1}3	872.42^{1}4	868.52^{1}0
19	976.64^{4}5*d*	973.75^{3}3*d*	920.70^{1}4	917.44^{1}5	867.65^{2}1*d*	863.70^{2}2*d*
20	977.28^{2}2*d*	974.32^{3}3*d*	918.65^{1}3	915.54^{1}3*d*	862.18^{2}3*d*	859.12^{1}1
21	977.95^{2}2	975.02^{4}4	916.39^{1}3	913.50^{1}4	857.32^{1}1	853.83^{2}4*d*
22	978.55^{2}0	975.66^{4}4*d*	914.09^{1}3	911.24^{1}4*d*	851.95^{1}0	849.12^{1}0
23	979.10^{4}5*d*	976.08^{2}4*d*	911.77^{1}4*d*	909.07^{2}5*d*	846.99^{2}2	844.11^{1}1
24	979.10^{4}5*d*	976.64^{4}5*d*	909.07^{2}5*d*	906.64^{2}5	841.86^{1}1	839.08^{1}1
25	979.34^{3}2	976.78^{4}3	906.64^{2}5	904.16^{2}3	836.50^{2}1	833.46^{2}1*d*
26	979.34^{3}2	976.78^{4}3	904.16^{2}5	901.47^{2}5	831.07^{1}0	——
27	979.34^{3}2	976.78^{4}3	901.47^{2}5	898.80^{2}2*d*	——	
28	979.10^{4}5*d*	976.78^{4}3	898.40^{1}2*d*	895.98^{1}0		
29	979.10^{4}5*d*	976.64^{4}5*d*	895.41^{1}5	893.02^{1}5*d*		
30	978.55^{2}0	976.08^{2}4*d*	892.12^{1}1	889.94^{2}4		
31	977.95^{2}2	975.66^{4}4*d*	888.94^{1}1	886.79^{1}1		
32	977.28^{2}2*d*	975.02^{4}4	885.60^{1}1*d*	883.61^{1}1		
33	976.64^{4}5*d*	974.32^{3}3*d*	882.24^{1}4*d*	880.31^{1}3		
34	975.66^{4}4*d*	973.75^{3}3*d*	878.70^{1}1	876.74^{2}2		
35	975.02^{4}4	972.78^{4}4	875.05^{1}1	873.22^{2}4		
36	973.75^{3}3*d*	971.81^{2}4*d*	871.40^{1}1	869.50^{1}5		
37	972.78^{4}4	970.72^{3}3	867.65^{2}1*d*	865.84^{1}2		
38	971.43^{2}3*d*	969.38^{3}3	863.70^{2}2*d*	862.18^{2}3*d*		
39	970.06^{1}1	967.96^{3}3	859.71^{1}2	858.14^{1}3*d*		
40	968.64^{1}1	966.43^{3}3	855.57^{1}2*d*	853.83^{2}4*d*		
41	966.95^{1}3*d*	964.92^{3}3	851.26^{1}1	849.92^{1}2*d*		
42	965.31^{1}4	963.42^{4}5*d*	846.99^{2}2	845.49^{1}1		
43	963.42^{4}5*d*	961.64^{4}5	842.52^{1}0	841.07^{1}2		
44	961.64^{4}5	959.79^{2}4*d*	838.04^{1}1*d*	836.50^{2}1*d*		
45	959.79^{2}4*d*	957.80^{1}2*d*	833.45^{2}1	831.97^{1}3		
46	957.34^{2}2*d*	955.62^{1}2	——	——		
47	954.84^{1}3*d*	953.43^{1}2				
48	952.79^{1}3	951.07^{1}3				
49	950.39^{1}3	948.56^{1}3				
50	947.63^{1}3	945.97^{1}2				
51	945.03^{1}3	943.32^{1}2				
52	942.13^{1}2	940.39^{2}4				
53	939.28^{2}4	——				

of arbitrariness in reporting the data in this way, that is in giving only lines assigned to the P, Q and R branches, it should be emphasized that every line of measurable intensity up to the head of the second band is accounted for and included in Table I. It is true that, due to the complexity of the structure blends of two or more lines are frequent, and the same wave-number often occurs several times in the table. It will be shown below, however,that this

TABLE I. (Continued)

R_2 *head*, λ2908.994			(1, 0) band R_1 *head*, λ2909.300		Q_1 *head*, λ2911.700	
K''	R_2	R_1	Q_2	Q_1	P_2	P_1
4			——	34,334.17^{1}2		
5			——	333.80^{2}3		
6			34,341.22^{2}2	333.05^{2}3		
7			339.19^{2}3	332.22^{1}1		
8			337.60^{1}2*d*	331.55^{2}4		
9			336.01^{2}3*d*	329.87^{2}2	——	——
10			333.80^{2}3	328.20^{2}2	34,306.27^{2}5	34,300.19^{1}1
11			331.55^{2}4	326.50^{1}3	301.07^{2}2	295.61^{2}5*d*
12			329.53^{2}4*d*	324.63^{2}4	296.22^{2}3*d*	291.08^{3}3
13			327.03^{1}3	322.53^{2}3*d*	291.08^{3}3	286.38^{1}1
14			324.63^{1}4	320.35^{2}5	285.68^{2}4	281.21^{2}4*d*
15	——		321.58^{1}2	317.95^{2}3*d*	280.69^{2}1	276.61^{2}4*d*
16	34,365.95^{2}5*d*	——	318.79^{1}3	315.24^{1}2	274.37^{2}4	270.55^{1}1
17	365.95^{2}5*d*	34,362.28^{2}5*d*	315.99^{1}3*d*	312.63^{2}5*d*	268.66^{1}1	265.24^{2}3*d*
18	365.28^{1}2*d*	362.28^{2}5*d*	312.63^{2}5*d*	309.33^{2}4	262.67^{1}0	259.39^{3}5*d*
19	364.71^{1}2	361.75^{2}2	309.33^{2}4	306.27^{2}5	256.56^{1}1	253.19^{1}2
20	363.87^{1}2	360.98^{1}2	305.76^{2}5	302.81^{2}3	250.38^{2}3	247.19^{1}3
21	363.09^{1}2	360.00^{1}3	302.07^{1}2	299.34^{1}2	244.12^{1}0	240.76^{1}3
22	361.75^{2}2	359.14^{2}4	298.27^{2}3*d*	295.61^{2}5*d*	237.27^{2}2	233.94^{1}1*d*
23	360.54^{1}1	357.94^{1}3	294.39^{1}2	291.68^{1}3	230.55^{1}3	227.55^{1}3
24	359.14^{2}4	356.50^{1}2	290.14^{1}2	287.66^{2}4*d*	223.56^{1}2	220.88^{2}3*d*
25	357.49^{1}3	354.95^{1}2*d*	285.68^{2}4	283.40^{1}3	216.56^{1}3	213.84^{2}3
26	355.71^{1}2	353.28^{1}3	281.21^{2}4*d*	278.83^{1}3	209.54^{1}1	207.11^{2}0
27	353.90^{1}2*d*	351.53^{2}3*d*	276.61^{2}4*d*	274.37^{2}4	202.56^{1}3*d*	199.42^{1}4
28	351.53^{2}3*d*	349.31^{2}4*d*	271.90^{1}3*d*	269.55^{2}4	194.40^{1}1*d*	192.13^{1}3
29	349.31^{2}4*d*	346.97^{2}4*d*	266.74^{1}3	264.60^{1}3	186.47^{1}2	184.38^{2}5
30	346.97^{2}4*d*	344.63^{1}3	261.49^{1}3	259.39^{3}5*d*	178.55^{2}2	176.55^{1}2*d*
31	344.16^{1}3	341.95^{1}2*d*	256.07^{1}2	254.15^{1}3	170.40^{1}0	168.30^{1}0
32	341.22^{2}2	339.19^{2}3	250.38^{2}3	248.57^{1}4	161.97^{2}3*d*	159.95^{1}1
33	338.27^{1}2	336.01^{2}3*d*	244.87^{1}3	243.04^{1}3	153.93^{2}1	151.83^{1}2
34	335.00^{1}2	333.05^{2}3	239.08^{1}1	237.27^{2}2	——	——
35	331.55^{2}4	329.53^{2}4*d*	233.09^{1}3*d*	231.26^{1}4		
36	328.20^{2}2	326.03^{1}2	226.88^{1}3	225.23^{1}2		
37	324.32^{2}4	322.53^{2}3*d*	220.88^{2}3*d*	218.89^{1}4*d*		
38	320.35^{2}5	317.95^{2}3*d*	213.84^{2}3	212.32^{1}3*d*		
39	316.30^{1}2	314.30^{1}2	207.11^{2}0	205.57^{1}5*d*		
40	311.79^{1}1	310.05^{1}2	200.24^{1}1	198.64^{1}2		
41	307.48^{1}2	305.76^{2}5	193.07^{1}3	191.70^{1}3		
42	302.81^{2}3	301.07^{2}2	185.77^{1}4	184.38^{2}5		
43	298.27^{2}3*d*	296.22^{2}3*d*	178.55^{2}2	177.13^{1}1		
44	293.03^{1}1	291.08^{3}3	170.90^{1}0	169.31^{1}3		
45	287.66^{2}4*d*	286.16^{1}3	163.17^{1}1	161.97^{2}3*d*		
46	282.46^{1}1	280.69^{2}1	155.40^{1}3	153.93^{2}1		
47	277.16^{1}0	275.06^{1}1	147.21^{1}0	145.97^{1}0		
48	270.96^{1}1	269.55^{2}4	——	——		
49	265.24^{2}3*d*	263.54^{1}1				
50	259.39^{3}5*d*	257.53^{1}1*d*				

does not materially detract from the certainty of our interpretation of the band structure. Following each wave-number in Table I, a superscript gives the number of times a given value appears, or in other words the number of lines of the band coinciding so closely as to be unresolved and measured as a single line. The last number gives a rough measure of the intensity, on a scale 0 to 5, from eye estimates made during the measurements. These are only strictly comparable for lines near together. The letter *d* indicates a particularly wide or diffuse line. Thus, for example, the line $R_1(26)$ in the (0, 0) band is given as 33,211.77[4] 3*d*, since it is a diffuse line formed by the near coincidence of $R_1(26)$, $R_2(28)$, $R_1(14)$, $R_2(10)$, and is of intensity 3 on the scale employed. Regularities in the intensities, as well as the significance of the designations R_2, R_1, K, etc., will be discussed below in connection with the quantum analysis.

INTERPRETATION OF THE DATA

Solution of band structure. In attacking the problem of sorting out the various branches, it was noticed from the outset that a short series of very strong lines appears in the region between the second and third heads of each band, and another at some distance beyond the third head (See Fig. 1). These lines are sharp only for a few members, becoming diffuse and soon separating into doublets at each end. Since the separation of adjacent lines in the first of these series is slightly less than that of the close double head, which is that formed by the branches R_2 and R_1 according to the provisional interpretation, it appeared that these strong lines must have about the separation of the so-called "natural" doublets of the R branch. These doublets are formed by pairs of lines with the same value of K[13] in the $^2\Pi$ state, and the components approach each other as the rotation increases to the point where the spin axis becomes coupled nearly as in Hund's case *b*.[6] With the doublets spaced so that the second component of one falls on the first component of the next, the above-mentioned series show exactly the aspect they should. This is the strongest of the series identified by Datta. Similarly, the second series is formed by an analogous coincidence in the doublets of the Q branch. With this opening, it was a simple matter to identify two series of doublets, those of the R and Q branches. The approximate assignment of rotational quantum numbers to these lines in the (0,0) band was then obtained in the following way. The first differences of the *mean* wave-numbers for the Q doublets were plotted against an arbitrary numbering, and extrapolated to zero spacing. This gives roughly the position of the band origin, ν_0, and a revised numbering of the Q lines, (starting with 1 at the point of convergence) which is correct to one or two units. The slope of the line is $2\,(B'-B'')$. Next, taking the mean values of the R doublets, we use the formula for the distance H from the (mean) R head to the origin.

$$H = B' - \frac{(B')^2}{B'-B''}\,.$$

One thus obtains approximate values of both B' and B'', and also an idea of the assignment of quantum numbers to the R lines, from the relation $K_{head} = B'/(B'-B'')$, to the nearest whole number. The method of working with mean values of the natural doublets recommends itself for such preliminary work, since these follow very nearly the simple relations in a band with singlet R, Q and P branches.

---

[13] K is used here for the resultant of Λ and N, where Λ measures the effective component of the resultant orbital angular momentum along the nuclear axis, and N the angular momentum of the nuclei (K formerly j_k, Λ formerly σ_k, N formerly m). Also J will here replace the former j (quantum number of the total angular momentum).

To be certain of the true K assignment, recourse must be had to the combination principle. To this end, the above process was repeated for the (1,0) band, and the R and Q series identified, with their approximate numbering. By suitably shifting the relative numbering in these series, both in the (0, 0) and (1, 0) bands, two sets of $R-Q$ differences were found which agreed throughout the observed range. These represent the combination differences $R_m(K)-Q_m(K+1)\cong\Delta_1F''(K)$, of the final state $v''=0$. In a $^2\Sigma$ state, one has[14]

$$\Delta_1F''(K)=2B''(K+1)+4D''(K+1)^3+\cdots, \tag{1}$$

where D can be approximated by the theoretical relations given on p. 327. Correcting for the cubic term, which is small, there results a series of quantities practically linear in K, which may be used to determine the final true assignment of K values. In agreement with the theoretical requirement for an odd molecule, the K values appeared definitely to be whole numbers. These $R-Q$ combination agreements obtained between the (0, 0) and (1, 0) bands were afterwards proved to be unique by the method of Pomeroy.[15] This is a systematic procedure for trying all possible relative numberings for the four branches,[16] which eliminates the possibility of a fortuitous agreement yielding false combination differences. Three other possible assignments were indeed found, with the short range of lines then available, but all of these gave a relative numbering far outside the range of possible error in the preliminary assignment reached by the method first described. Considering finally the (0, 1) band, it was found that with but a slight shift in the preliminary numbering, satisfactory equality could be obtained with the differences $R_m(K)-Q_m(K)=\Delta_1F'_m(K)$ from the (0, 0) band.

In identifying the remaining lines of the bands, a convenient procedure described by Loomis and Wood[17] was followed. Having the lines of a portion of a given branch, one derives an empirical formula in K to fit the wave-numbers of these members, using again the mean value of each doublet. The deviations of all observed lines from this equation are then plotted; at least of all which lie within a few cm^{-1} on either side of each calculated value. Such a diagram is shown in Fig. 2 for the Q lines of the (0, 0) band. The series stand out clearly among the extraneous lines, and the proper line to choose in each case is apparent. The method has the added advantage that any other series with approximately the same spacing as those used, such as the so-called "satellite" series, will reveal their presence. By this means, the Q branches were extended to small values of K, the low-frequency components converging in the third head, and the high-frequency components extending into the comparatively simple portion beyond this head. The low K lines of the R branches could then be found by adding the appropriate combination

---

[14] This expression for Δ_1F'', the difference between adjacent rotational terms of the lower state, is derived directly from the term formula, Eq. (3) below.

[15] W. C. Pomeroy, Phys. Rev. **29**, 59 (1927).

[16] I am indebted to Mr. S. W. Nile, New York University, for performing this lengthy calculation.

[17] F. W. Loomis and R. W. Wood, Phys, Rev. **32**, 223 (1928).

differences $\Delta_1 F''(K)$, computed from Eq. (1), to the mean values $Q_m(K+1)$. Adding and subtracting half the doublet separation for $Q(K+1)$, the R lines going up to the head were identified as a series of weak lines not previously assigned. The location of this series was clearly not that to be expected if the doubling of $R(K)$ was assumed to be the same as that of $Q(K)$. This is a proof that the large doubling is in the initial state, and that the transition is $^2\Pi \rightarrow {}^2\Sigma$, and not $^2\Sigma \rightarrow {}^2\Pi$. This statement will be evident if one refers to the energy level diagram of Fig. 3.

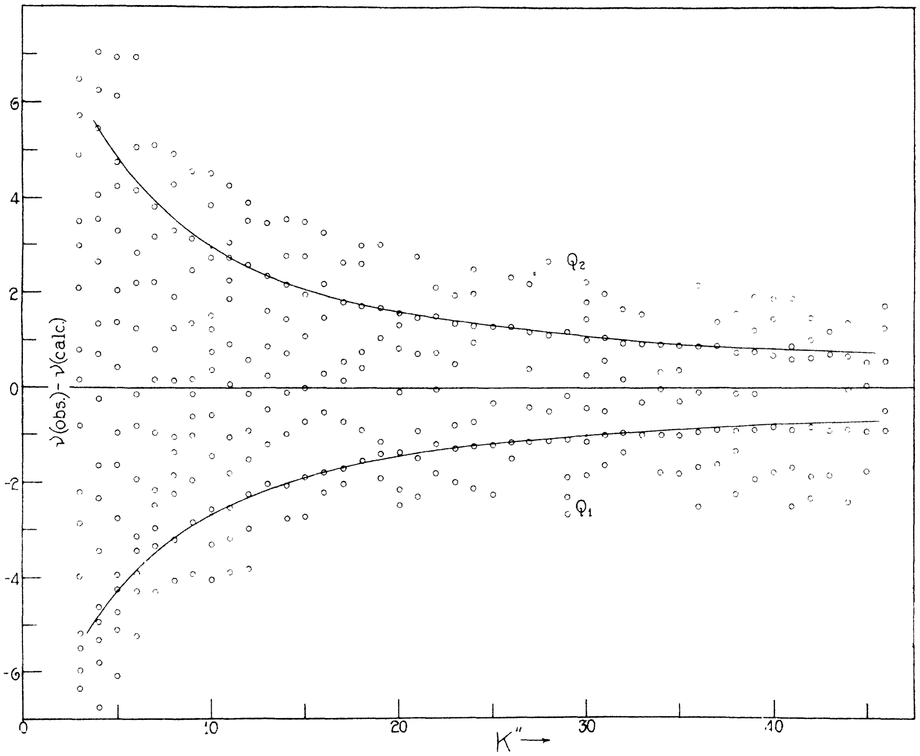

Fig. 2. Deviations of lines in the (0, 0) band from the approximate formula for the mean wave-numbers of the Q doublets: $Q_m(K) = \nu_0 - B' + (B'-B'')\ (K+\frac{1}{2})^2 + (D'-D'')\ (K+\frac{1}{2})^4 = 33{,}185.80 - 0.0685(K+\frac{1}{2})^2 - 0.0920 \times 10^{-6}\ (K+\frac{1}{2})^4$. The curves give the deviations of the theoretical values of $Q(K)$, calculated by Eq. (11).

The R branches are comparatively free from overlapping by extraneous lines, but their extension to values of K lower than that of the head could not be satisfactorily done in the weaker bands (0, 1) and (1, 0), especially the latter, where the value of K_{head} is smallest. Graphs of the type shown in Fig. 2 were used to identify the Q and P branches in all three bands. The preliminary equation for finding the P branches was based on the aproximate relation

$$P_m(K) = Q_m(K-1) - [R_m(K-1) - Q_m(K)]. \qquad (2)$$

This is strictly true only in the absence of the well-known Λ-type doubling associated with $^2\Pi$ states. A systematic deviation from the predicted positions of the P lines was in fact found, of nearly the same magnitude for the components P_2 and P_1. The observed lines were slightly displaced toward lower frequencies from the values calculated by Eq. (2).

Analysis of rotational terms. The lines given in Table I comprise six branches for each band, three of which, R_1, Q_1 and P_1, are to be correlated with terms of the initial and final states in which the spin vector, $S=1/2$, when completely uncoupled from the nuclear axis, stands parallel to the resultant vector K of the orbital and nuclear angular momenta. Similarly, for R_2, Q_2 and P_2, S is anti-parallel to K in both states. In the lower state, $^2\Sigma$, there is no component, Λ, of the orbital angular momentum along the molecular axis, and hence no interaction of the spin with this axis, even at very low values of K. The rotational terms may then be represented by

$$F_i(J)=BK(K+1)+D[K(K+1)]^2+\cdots. \tag{3}$$

In this case each level is a degenerate pair, $F_2(K-1/2)$ coinciding with F_1 $(K+1/2)$, where F_1 and F_2 designate terms having S parallel and antiparallel to K, respectively. If this degeneracy is removed by the rotation, we have ρ-type doubling, but in the present case no evidence for this doubling was found, as explained below, under *Intensities.*

In the initial state, $^2\Pi$, the situation is more complicated. At high speeds of rotation, the condition is almost the same as in the $^2\Sigma$ case, levels of the same K coming close together. In Fig. 3, the tendency of these levels to approach each other is evident, even when K is relatively small. With decreasing K, the corresponding levels diverge more and more, as the interaction of the spin with the molecular axis beomes stronger. In the limit of no rotation if the doublet is normal, S is anti-parallel to Λ for F_1 terms ($^2\Pi_{1/2}$), and parallel for $F_2(^2\Pi_{3/2})$. If it is inverted, S is parallel to Λ for F_1 terms ($^2\Pi_{3/2}$) and antiparallel for $F_2(^2\Pi_{1/2})$. In either case the set of lower energy is designated F_1. Two methods are available for distinguishing a normal from an inverted doublet. There should be more missing lines in the $^2\Pi_{3/2}$ than in the $^2\Pi_{1/2}$ sub-band. In the present case these could not be determined, due partly to the numerous cases of superposition, and partly to the faintness of the first few lines in a branch. An alternative criterion is available in the magnitude of the Λ-type doubling. In case a, this is always much larger for $^2\Pi_{1/2}$ than for $^2\Pi_{3/2}$.[18] It was impossible in our case to detect this doubling for low values of K, and at larger values the type of coupling approaches case b rapidly. Van Vleck has shown[18] that in the strict case b the Λ-type doubling should be equal for $^2\Pi_{1/2}$ and $^2\Pi_{3/2}$. That this is not exactly true in the BeF bands, even for very large K, can be most directly shown by comparing the natural doublet separation for $Q(K)$ with that for $R(K-1)$and $P(K+1)$. The Q branch separations are noticeably smaller, which shows that the Λ-type doubling is greater in the F_1' states (see Fig. 3). The difference is not great, however, and is only

---

[18] J. H. Van Vleck, Phys. Rev. **33**, 467 (1929). R. S. Mulliken, Phys. Rev. **33**, 507 (1929).

considerable for high K values, as will be seen in Fig. 4, which represents graphically the course of these natural doublet separations. In the absence of confirmatory evidence from the missing lines, it seemed best to assume that the $^2\Pi$ state is normal.

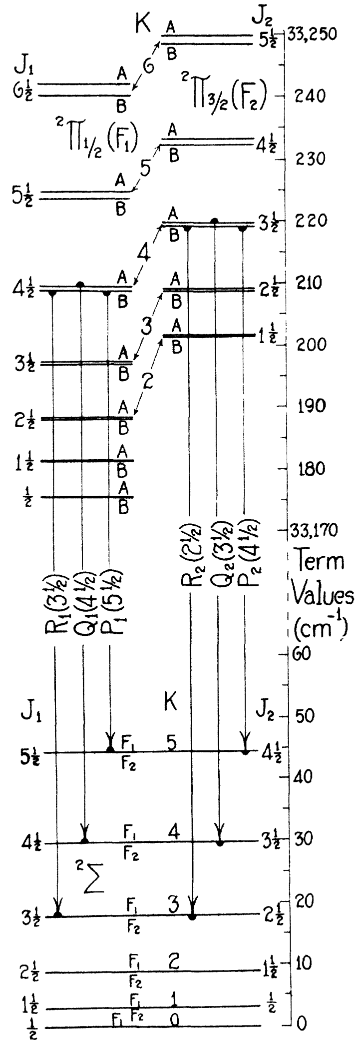

Fig. 3. First few rotational terms in the initial and final states $v=0$, drawn to scale according to Eqs. (3) and (4). The transitions shown by the vertical arrows give the natural doublets $R(K-1)$, $Q(K)$ and $P(K+1)$, (here $K=4$) which have the same doublet separation, except for slight differences in the Λ-type doubling for $F_1'(K)$ and $F_2'(K)$. The latter doubling, to be visible, is magnified 100-fold.

The effect of the transition from case a at low rotational speeds to case b at high speeds upon the energy formula for doublet states was first studied quantitatively by Kemble.[19] The resulting equations were tested with the OH

---

[19] E. C. Kemble, Phys. Rev. **30**, 387 (1927).

bands, and gave excellent agreement except at the lowest values of K. Slight discrepancies were to be expected, because the formulas were based on the old quantum theory. More recently, Hill and Van Vleck,[20] using the new mechanics, have obtained a convenient closed formula for the energy throughout the transition from case *a* to case *b*, applicable to both normal and inverted doublets. Aside from their statement that somewhat better agreement with experiment is obtained in the case of OH than found by Kemble, this formula appears not to have been applied in any specific case. It is therefore desirable to see how well it is capable of giving the observed rotational terms in Be F. Denoting by λ the ratio $\Delta E/B\Lambda$, and introducing the term in $D[K(K+1)]^2$ appropriate to case *b* (since this is appreciable only at higher values of K) the equations of Hill and Van Vleck may be written

$$\begin{aligned} F_2(J) &= B(K^2-\Lambda^2)+\frac{B}{2}[4K^2+\lambda(\lambda-4)\Lambda^2]^{1/2}+D[K(K+1)]^2+\cdots \\ F_1(J-1) &= B(K^2-\Lambda^2)-\frac{B}{2}[4K^2+\lambda(\lambda-4)\Lambda^2]^{1/2}+D[K(K-1)]^2+\cdots . \end{aligned} \tag{4}$$

The J in each case is that appropriate to the value of K in the same equation, that is, $J_2=K-1/2$, $J_1=K+1/2$. For a $^2\Pi$ state, $\Lambda=1$ always. The constant $B=h/8\pi^2Ic$ is best determined from the initial state combination differences at relatively high K, where case *b* is approximated. Thus, one has

$$\Delta_1F_m'(K)=2B'(K+1)+4D'(K+1)^3+\cdots . \tag{5}$$

Taking $\Delta_1F'_m(K)$ as the mean of the combination differences $R_m(K)-Q_m(K)$ and $Q_m(K+1)-P_m(K+1)$, to eliminate the effect of Λ-type doubling, the constants[21] $B^{(0)\prime}$ and $B^{(1)\prime}$, were evaluated by least squares from the ΔF's between $K=20$ and 30. For this purpose, the effect of the term in $(K+1)^3$ was first allowed for by using the accurate values of $D^{(0)\prime}$ and $D^{(1)\prime}$ obtained from the theoretical relations[22]

$$\begin{aligned} D^{(v)} &= D_e+\beta(v+\tfrac{1}{2}) \\ D_e &= -4B_e^3/\omega_e^2 \\ \beta &= \frac{\alpha^2}{6\omega_e}+\frac{20\alpha B_e^2-32x_eB_e^3}{\omega_e^2} . \end{aligned} \tag{6}$$

The equation for β is taken from Kemble's work,[23] and is in a more convenient form than that given by Pomeroy.[15] The ω_e and x_e were taken from Jevons' work,[5] and α was approximated from preliminary results. An analogous com-

---

[20] E. L. Hill and J. H. Van Vleck, Phys. Rev. **32**, 250 (1928).

[21] The vibrational quantum number v to which a constant refers will be indicated as a superscript, in parentheses.

[22] The subscript e indicates that the constant refers to the *equilibrium* position of the nuclei ($v=-\frac{1}{2}$).

[23] E. C. Kemble, Jour. Opt. Soc. Am. **12**, 1 (1926). The possibility of getting this convenient expression for β was kindly called to my attention by Prof. R. T. Birge.

putation with $\Delta_1 F''$, using Eq. (1), gave the constants $B^{(0)''}$ and $B^{(1)''}$ of the final state.

Since it was impossible to obtain observed values of the separations of the lowest levels, it was necessary to choose a value for λ such that Eqs. (4) fit the data for higher K most exactly. If this can be done, we have the electronic difference in the upper state for zero rotation, ΔE, since by definition $\lambda = \Delta E/B$. Instead of calculating the actual $F(J)$ values, it is more convenient to use the expression derived from Eqs. (4) for the natural doublet separation:[24]

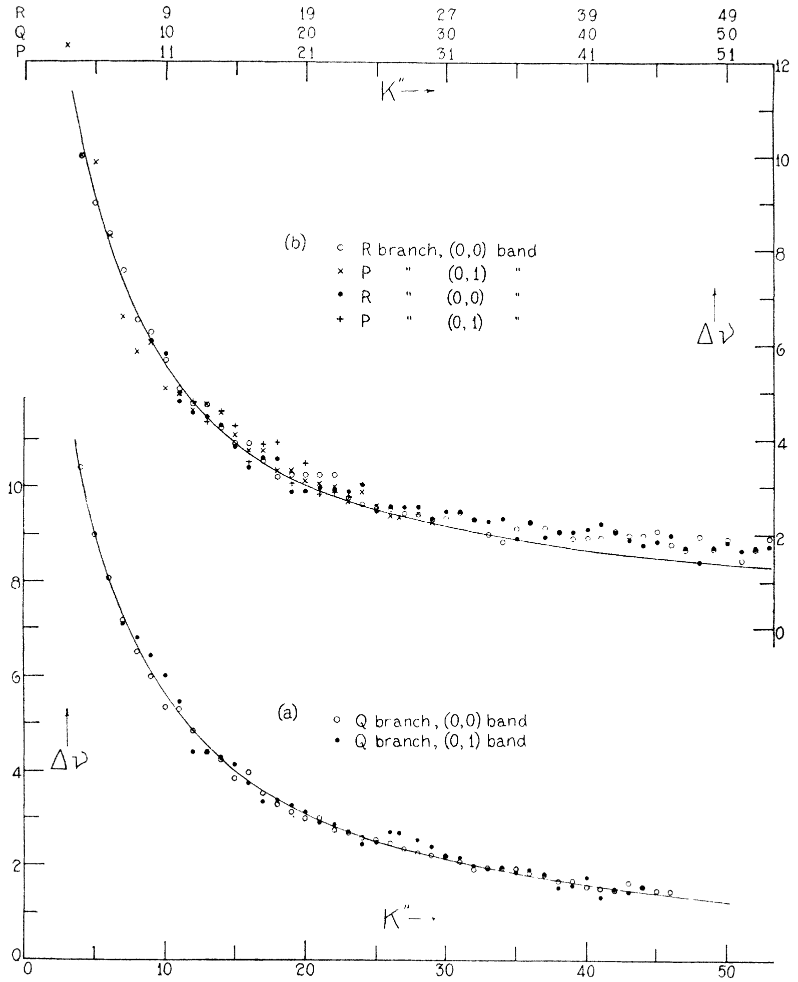

Fig. 4. Separation of the natural doublets as a function of rotational quantum number. In (a) the curve gives the theoretical separations from Eq. (7). The curve in (b) gives the best representation of the empirical separations in the Q branches, to show their divergence from those in the R and P branches at high values of K.

---

[24] The equation for Δ given by Hill and Van Vleck applies not to the actual doublets, but to a mean value of the separation for two adjacent ones.

$$\Delta = F_1'(K) - F_2'(K) = B'\left[\tfrac{1}{2}\left\{4K^2+\lambda(\lambda-4)\right\}^{1/2}+\tfrac{1}{2}\left\{4(K+1)^2+\lambda(\lambda-4)\right\}^{1/2}\right.$$
$$\left. -2(K+\tfrac{1}{2})\right] \cong B'\left[\left\{4(K+\tfrac{1}{2})^2+\lambda(\lambda-4)\right\}^{1/2}-2(K+\tfrac{1}{2})\right]. \quad (7)$$

The best representation of Δ from the Q branches, shown graphically in Fig. 4(a) is obtained with $\lambda = +15.667$, assuming a normal doublet. If the doublet is taken as inverted, an equally good fit is obtained with $\lambda = -11.667$. With $B' = 1.4108$ (see p. —), this gives for the electronic separation in the $^2\Pi$ state $\Delta E = +22.10$ cm^{-1} if it is normal, -16.46 if inverted. A change of ± 0.1 cm^{-1} in these quantities makes the agreement with the observed Δ curves definitely less exact.

The rotational terms, $F(J)$ are not found directly from the spectrum, but only their differences, ΔF. Table II contains these quantities for all cases in which agreements between different sets are to be expected. Strict equality should only be found for corresponding differences in two bands with a common vibrational state, for example $R_2(K) - Q_2(K)$ in the (0, 0) and (0, 1) bands. The agreement of the differences $R-Q$ with $Q-P$ is only approximate, due to the Λ-type doubling in the initial state. It seemed best, for purposes of comparison with the theory, to eliminate the effect of this

TABLE II. *Agreements in the combination differences.*

K	$R_2(K)-Q_2(K)$ $=\Delta_1F_2'-\delta F_2(K+\frac{1}{2})$		$R_1(K)-Q_1(K)$ $=\Delta_1F_1'-\delta F_1(K+\frac{1}{2})$		$R_2(K)-Q_2(K+1)$ $=\Delta_1F_2''-\delta F_2(K+1)$		$R_1(K)-Q_1(K+1)$ $=\Delta_1F_1''-\delta F_1(K+1)$	
	(0,0)	(0,1)	(0,0)	(0,1)	(0,0)	(1,0)	(0,0)	(1,0)
17	50.4	50.5	50.7	50.3	52.9	53.3	53.0	53.0
18	53.4	53.0	53.4	53.4	56.0	56.0	55.9	56.0
19	56.0	56.0	55.9	56.3	58.9	58.9	58.6	58.9
20	58.8	58.6	58.6	59.2	61.8	61.8	61.6	61.6
21	61.8	61.6	61.6	61.5	64.8	64.8	64.3	64.4
22	64.4	64.5	64.3	64.4	67.7	67.4	67.6	67.5
23	67.1	67.3	67.1	67.0	70.4	70.4	70.4	70.3
24	69.8	70.0	69.8	70.0	73.2	73.5	73.2	73.1
25	72.5	72.7	72.5	72.6	76.0	76.3	76.0	76.1
26	75.2	75.2	75.3	75.3	79.1	79.1	79.0	78.9
27	78.0	77.9	77.9	78.0	81.9	82.0	81.8	81.9
28	80.6	80.7	80.5	80.8	84.6	84.8	84.5	84.7
29	83.5	83.7	83.4	83.6	87.7	87.8	87.6	87.6
30	86.5	86.4	86.2	86.1	90.7	90.9	90.3	90.5
31	89.1	89.0	88.7	88.9	93.6	93.8	93.1	93.4
32	91.7	91.7	91.6	91.4	96.2	96.3	96.2	96.2
33	94.2	94.4	94.3	94.0	98.9	99.2	99.0	98.7
34	97.1	97.0	96.9	97.0	101.9	101.9	101.7	101.8
35	99.8	100.0	99.5	99.6	104.8	104.7	104.3	104.3
36	102.5	102.4	102.2	102.3	107.6	107.3	107.2	107.1
37	105.1	105.1	104.8	104.9	110.5	110.8	110.1	110.2
38	107.8	107.7	107.5	107.2	113.1	113.2	112.8	112.4
39	110.4	110.4	110.1	109.8	115.9	116.1	115.6	115.7
40	113.1	113.0	112.7	112.6	118.8	118.7	118.4	118.4
41	115.9	115.7	115.4	115.0	121.7	121.7	121.1	121.4
42	118.5	118.3	118.0	117.9	124.3	124.3	124.0	123.9
43	121.0	120.9	120.7	120.6	127.1	127.4	126.7	126.9
44	123.6	123.6	123.1	123.3	130.0	129.9	129.4	129.1

TABLE II. (Continued)

K	$Q_2(K+1)-P_2(K+1)$ $=\Delta_1F_2'+\delta F_2(K+\frac{1}{2})$		$Q_1(K+1)-P_1(K+1)$ $=\Delta_1F_1'+\delta F_1(K+\frac{1}{2})$		$Q_2(K)-P_2(K+1)$ $=\Delta_1F_2''+\delta F_2(K+1)$		$Q_1(K)-P_1(K+1)$ $=\Delta_1F_2''+\delta F_1(K+1)$	
	(0,0)	(0,1)	(0,0)	(0,1)	(0,0)	(1,0)	(0,0)	(1,0)
9	27.8	....	28.5	....	29.6	29.7	29.6	29.7
10	31.0	....	30.8	....	32.5	32.7	32.3	32.7
11	33.8	33.8	33.9	34.4	35.6	35.3	35.2	35.4
12	36.7	36.7	36.9	37.1	38.7	38.5	38.5	38.3
13	39.2	39.3	39.7	39.4	41.3	41.4	41.7	41.3
14	41.7	42.4	42.4	42.8	44.0	43.6	44.3	43.7
15	45.1	44.8	45.2	45.4	47.0	47.2	47.3	47.4
16	47.8	47.7	48.1	47.9	50.5	50.1	50.3	50.0
17	50.5	50.3	51.0	50.8	53.1	53.3	53.3	53.2
18	53.6	53.1	53.8	53.7	56.2	56.1	56.3	56.1
19	56.2	56.5	56.5	56.4	59.0	59.0	59.3	59.1
20	59.0	59.1	59.2	59.7	62.0	61.6	62.1	62.1
21	61.9	62.1	62.2	62.1	64.9	64.8	64.9	65.4
22	64.5	64.8	64.8	65.0	67.8	67.7	68.0	68.1
23	67.4	67.2	67.5	67.6	70.7	70.8	70.8	70.8
24	70.1	70.1	70.5	70.7	73.6	73.6	73.9	73.8
25	73.0	73.1	73.2	....	76.6	76.1	76.7	76.3
26	75.6	....	75.7	....	79.5	78.7	79.4	79.4
27	78.3	....	78.4	....	82.5	82.2	82.2	82.2
28	81.1	....	81.3	....	85.1	85.4	85.2	85.2
29	83.9	....	84.0	....	88.1	88.2	88.2	88.1

TABLE II. (Continued)

K	$R_2(K)-P_2(K)$ $=\Delta_2F'_{2B}$		$R_1(K)-P_1(K)$ $=\Delta_2F'_{1B}$		$R_2(K-1)-P_2(K+1)$ $=\Delta_2F_2''$		$R_1(K-1)-P_1(K+1)$ $=\Delta_2F_1''$	
	(0,0)	(0,1)	(0,0)	(0,1)	(0,0)	(1,0)	(0,0)	(1,0)
12	70.3	70.2	70.5	70.7	74.2	....	74.1	....
13	76.0	76.0	76.4	76.5	79.9	....	79.9	....
14	81.4	81.2	82.2	81.7	85.4	....	85.7	....
15	86.8	86.5	87.4	87.7	91.5	....	91.6	....
16	92.4	92.7	93.0	93.3	97.6	97.3	97.4	....
17	98.2	98.3	98.7	98.2	103.1	103.3	103.4	102.9
18	103.9	103.2	104.4	104.3	109.1	109.4	109.3	109.1
19	109.6	109.0	109.7	110.0	115.0	114.9	115.1	115.1
20	115.1	115.1	115.1	115.6	120.9	120.6	120.7	121.0
21	120.9	120.6	120.7	121.2	126.7	126.6	126.5	127.0
22	126.2	126.6	126.5	126.5	132.6	132.5	132.4	132.4
23	131.5	132.1	131.9	132.0	138.4	138.2	138.3	138.3
24	137.1	137.2	137.2	137.6	144.0	144.0	144.3	144.1
25	142.6	142.8	143.0	143.3	149.8	149.6	149.8	149.4
26	148.3	148.3	148.5	....	155.5	154.9	155.4	155.5
27	153.6	....	153.6	....	161.3	161.3	161.2	161.2
28	158.9	....	158.9	....	167.0	167.4	167.0	167.1
29	164.6	....	164.7	. . .	172.7	173.0	172.6	172.8

doubling by defining the ΔF's in terms of the centers of the doublet levels. Reference to Fig. 3 will show that to obtain these ΔF's, the differences between actual lines must be corrected by an amount proportional to the combination defect $[R(K)-Q(K+1)]-[Q(K)-P(K+1)]$, which we will call $2\delta F$. According to the theory,[18] the Λ-type doubling, and hence the combination defect, should be proportional to $(J+\frac{1}{2})^2$. Graphs of $2\delta F$ against J for F_1' and F_2' states gave curves similar to that obtained by Loomis and Wood[17] for the Na_2 bands, in which the defect could be satisfactorily represented as proportional to $(J+\frac{1}{2})^2$. Hence a simple method of taking the Λ-type doubling into account in the energy formulas is to give slightly different values of B to the F_A and F_B levels. Their difference can be found from the combination defect by the relation[17]

$$\begin{aligned} 2\delta F &= [F_A'(J+1)-F_B'(J+1)]+[F_A'(J)-F_B'(J)] \\ &\cong 2[F_A'(J+\tfrac{1}{2})-F_B'(J+\tfrac{1}{2})]=2(B_A'-B_B')(J+\tfrac{1}{2})^2. \end{aligned} \tag{8}$$

The values of $B_A'-B_B'$ obtained in this way were, for F_1' states, $+0.00046$, and for F_2', $+0.00028$. The corrections, δF_1 and δF_2, to be applied to the combination differences to obtain the quantities $\Delta_1 F'$ are indicated above each column in Table II.

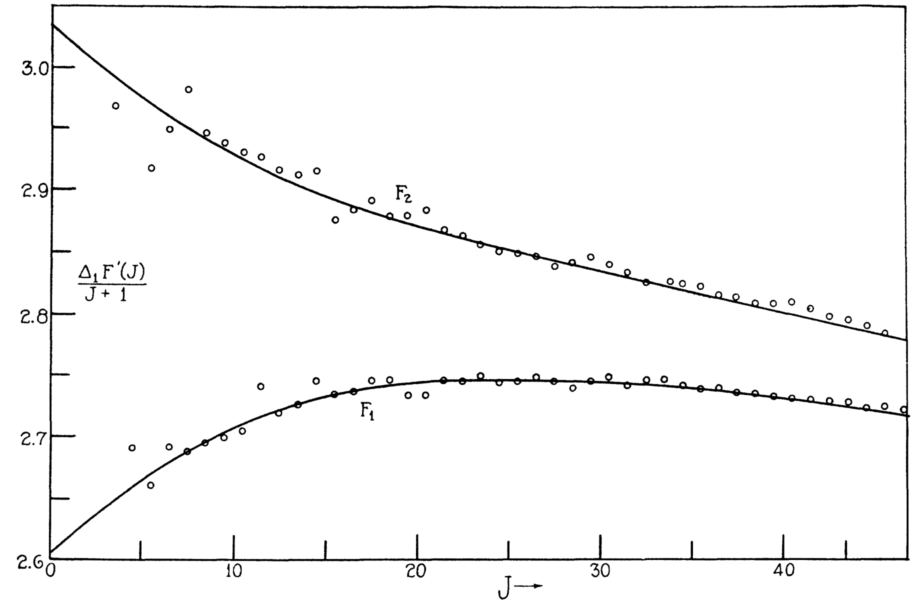

Fig. 5. Comparison of $\Delta_1 F'(J)/(J+1)$ with the theoretical curves (Eq. (10)). Data from the (0, 0) band.

The formula for $\Delta_1 F'$ may be found from Eqs. (4) as follows:

$$\begin{aligned} \frac{dF_i(J)}{dJ} &= \Delta_1 F_i(J-\tfrac{1}{2}) = 2B'(J+\tfrac{1}{2})\left[1\pm(4(J+\tfrac{1}{2})^2+\lambda(\lambda-4))^{-1/2}\right] \\ &\quad +4D'(J+\tfrac{1}{2}\pm\tfrac{1}{2})^3+\cdots. \end{aligned} \tag{9}$$

The upper sign applies to F_2 and the lower to F_1. This formula was tested in several cases, and agreed with the observed ΔF's within a few hundredths cm^{-1}. For a graphical comparison of the theory with the empirical results, it is more convenient to divide the ΔF's throughout by $(J+\frac{1}{2})$. Thus, to a close approximation

$$[\Delta_1 F_i'(J-\tfrac{1}{2})]/(J+\tfrac{1}{2})=2B'[1\pm\{4(J+\tfrac{1}{2})^2+\lambda(\lambda-4)\}^{-1/2}]+4D'(J+\tfrac{1}{2}\pm\tfrac{1}{2})^2. \quad (10)$$

In Fig. 5 are plotted the observed quantities $\Delta F/(J+1)$ against J, and the curve represents the theoretical values from Eq. (10). Although systematic discrepancies are evident, especially at high J, it is probable that these could be somewhat reduced by slight adjustments of the constants. This was not attempted, but it is clear that the theory accounts remarkably well for the rather complicated variation of the ΔF's. Not only do the two sets draw together in the proper way, but they show the expected downward trend at large J values due to the term in D'.

The term-formulas (4) are surprisingly simple, considering the complexity of the uncoupling phenomenon involved. They permit the representation of all the lines of a complex band of this kind by comparatively compact and convenient formulas. Taking Eqs. (3) for the terms of the lower state, and Eqs. (4) for those of the upper, and forming the appropriate differences for the several branches, one obtains expressions of the form:

$$\nu=a+bK+c/2[4K^2+\lambda(\lambda-4)]^{1/2}+dK^2+eK^3+fK^4. \quad (11)$$

TABLE III. *Values of coefficients for each branch.*

Lines	a	b	c	d	e	f
$R_2(K-1)$	ν_0-B_{2B}'	B''	B_{2B}'	$B_{2B}'-B''$	$2(D'+D'')$	$D'-D''$
$R_1(K-2)$	$\nu_0-B_{1B}'-2B''$	$3B''$	$-B_{1B}'$	$B_{1B}'-B''$	$-2(D'-3D'')$	$D'-D''$
$Q_2(K)$	ν_0-B_{2A}'	$-B''$	B_{2A}'	$B_{2A}'-B''$	0	$D'-D''$
$Q_1(K-1)$	ν_0-B_{1A}'	B''	$-B_{1A}'$	$B_{1A}'-B''$	0	$D'-D''$
$P_2(K+1)$	$\nu_0-B_{2B}'-2B''$	$-3B''$	B_{2B}'	$B_{2B}'-B''$	$2(D'-3D'')$	$D'-D''$
$P_1(K)$	ν_0-B_{1B}'	$-B''$	$-B_{1B}'$	$B_{1B}'-B''$	$-2(D'+D'')$	$D'-D''$

The coefficients to be used for each branch are given in Table III. The origin, ν_{00} of the (0, 0) band was found by applying these equations to several lines of each branch, the average of a number of consistent values being 33,187.21 cm^{-1}. Eq. (11), taken in connection with our final values of the constants, listed below, represents all the lines of the (0, 0) band quite accurately, the largest consistent deviation being about 0.2 cm^{-1}. Errors of this size would not be noticeable in a diagram on the scale of that in Fig. 1. Small systematic trends are apparent, however, when the lines are represented graphically by the method illustrated in Fig. 2. Nevertheless, the formulas reproduce the observed lines to the same order of accuracy as do the more familiar ones applicable to bands of simpler structure.

The molecular constants resulting from the present study of the band structure are given in Table IV. All are expressed in cm^{-1} units.

TABLE IV. *Molecular constants.*

Initial state, $^2\Pi$ (normal)	Final state, $^2\Sigma$
$\Delta E=22.10$	
$B_{1A}^{(0)}=1.41083$	
$B_{1B}^{(0)}=1.41037$	$B^{(0)}=1.47928$
$B_{2A}^{(0)}=1.41074$	
$B_{2B}^{(0)}=1.41046$	
$\alpha=B^{(0)}-B^{(1)}=0.01610$	0.01685
$D^{(0)}=-8.301\times10^{-6}$	-8.209×10^{-6}
$\beta=D^{(1)}-D^{(0)}=1.060\times10^{-8}$	2.903×10^{-8}

Defining B_e as the value of $h/8\pi^2 I_e c$ for the non-vibrating molecule, we have $B^{(v)}=B_e-\alpha(v+\frac{1}{2})$, whence $B_e=B^{(0)}+\alpha/2=1.48770$ in the lower state. Using the relation $I_e=27.66/B_e$ given by Birge,[25] the equilibrium value of the moment of inertia in the less excited state becomes $(18.59\pm0.03)\ 10^{-40}$ g cm^2, and the corresponding internuclear distance 1.357A. In the more excited state, these quantities are, respectively, $(19.50\pm0.03)\ 10^{-40}$ g cm^2 and 1.390A.

Intensities. The intensity in each branch rises to a maximum at about $K=20$, and then falls off slowly in the usual way. On our plates, the first few lines were too faint to be observed. The two components of each natural doublet are, as far as can be judged, of equal intensity. Because of the great amount of overlapping in the P branches and the outer part of the Q branches it is difficult to compare the relative intensities of the various branches. By considering only the weaker lines in the regions where blends are frequent, an approximation can be made, however. The P branches have about the same intensity as the R—perhaps slightly less. The Q lines are much stronger, with about twice the intensity of the R lines of the same rotational quantum number.

Mulliken's scheme[6] for $^2\Pi\rightarrow{}^2\Sigma$ transitions predicts certain satellites of the strong branches, and two further branches, for which $\Delta K=\pm2$. All of these should be relatively weak when $\Delta E/B$ is small. In the absence of ρ-type doubling in the final state, his satellites $^RQ_{21}$ and $^QP_{21}$ coincide with the strong branches R_2 and Q_2 respectively. Similarly, $^QR_{12}$ and $^PQ_{12}$ coincide with Q_1 and P_1. Our failure to observe these satellites is the most important evidence for the absence of appreciable ρ-type doubling in the $^2\Sigma$ state of BeF. Of Mulliken's double R- and double P-form branches, which may be called S_{21} and O_{12}, the former is definitely absent, and therefore almost certainly the latter as well. Our graphical investigations by the method of Fig. 2 show no evidence for the presence of the satellites Q_{2B2A} and Q_{1B1A}, which violate the selection principle for Λ-type doubling, but which are, however, found in the OH bands.

Vibrational structure. Jevons[5] has derived the following equations to represent the heads of some 45 bands of this system.

---

[25] R. T. Birge, Phys. Rev. Supplement **1**, 62 (1929).

R_2 *heads:* $\nu = 33{,}217.3 + 1153.3v' - 5.88v'^2 - 1247.1v'' + 11.21v''^2 - 4.92v'v''$
R_1 *heads:* $\nu = 33{,}214.3 + 1153.9v' - 5.67v'^2 - 1247.1v'' + 11.50v''^2 - 5.36v'v''$
Q_1 *heads:* $\nu = 33{,}179.9 + 1163.8v' - 8.78v'^2 - 1256.5v'' + 9.12v''^2$.

The coefficients in the third equation, except the constant term, apply equally well to the band origins, since the head of the Q_1 branch occurs at a very small value of K. Assuming that the vibrational constants are the same in $^2\Pi_{3/2}$ and $^2\Pi_{1/2}$, the variation with v of the distance from the Q_1 head to the origin is probably negligible. Inserting the constant, ν_{00}, evaluated above, the equation for origins becomes

$$\nu_0 = 33{,}187.21 + 1163.8v' - 8.78v'^2 - 1256.5v'' + 9.12v''^2 \tag{12}$$

The vibration frequency for infinitesimal amplitudes is, accordingly, $\omega_e = \omega^{(0)} + x\omega^{(0)} = 1265.62$ in the final state, and 1172.58 in the initial state. The electronic frequency, ν_e of the system-origin is obtained as the constant term when Eq. (12) is transformed to express ν_0 as a function of $(v+\frac{1}{2})$. We find $\nu_e = 33{,}233.61$.

Morse[26] has recently found an empirical relation connecting the constants $\omega^{(0)}$ and $r^{(0)}$, which is useful as a check on the correctness of our analysis. According to this rule, $\omega^{(0)}r^{(0)} = 3000 \pm 120\text{A}^3/\text{cm}$. In the present case the product is 3159 and 3176 in the upper and lower states, respectively. Another important rule, due to Birge[27] requires that $2xB^{(0)}/\alpha = 1.4 \pm 0.2$. From our constants, this ratio for BeF is 1.32 in the upper state, and 1.27 in the lower.

CONCLUSIONS

This is the first analysis of a band structure of the contracting doublet type in a spectrum other than that of a diatomic hydride. Due to the much closer spacing of the lines (the moment of inertia is 13 times that of OH), the actual resolving power available was not far above the mimimum required for an unambiguous proof of the structure by the application of the combination principle. In view of the various agreements with the theory, and especially of the graphical proofs of the reality of the different line series, it is thought that our results are justified in all their more essential respects. Several investigators[1,5] have drawn conclusions concerning the electronic states of other alkaline earth halides from a study of the positions and intensities of the heads in the numerous band systems of these molecules. As stated above, these systems appear to be beyond the reach of our present spectrographs, as far as the rotational structure is concerned. It should be emphasized that bands due to entirely different types of electronic transitions may show an almost identical gross structure. For example, the BeF bands described here show very nearly the same relative spacing and intensity of the three heads in each band as do the blue-green TiO bands recently analysed by Christy,[28] although the states involved are even of a different mul-

---

[26] P. M. Morse, Phys. Rev. **34**, 57 (1929).

[27] R. T. Birge, Phys. Rev. **31**, 919 (1927) (Abstract).

[28] A Christy, Phys. Rev. **33**, 701 (1929).

tiplicity; the transition is $^3\Pi \rightarrow ^3\Pi$. Therefore, unless one brings every available type of evidence to bear, it seems that conclusions based on a study of the band heads alone must be regarded as highly speculative.

The $^2\Pi \rightarrow ^2\Sigma$ system of BeF constitutes the entire known spectrum of this molecule. Although it has not as yet been obtained in absorption, it appears probable, from analogy with the iso-electronic molecule CN, that the $^2\Sigma$ state is the normal electronic configuration. The band systems in the visible region due to a number of other alkaline earth halides have been found in absorption.[29] Mulliken[30] has given a provisional assignment of quantum numbers to the individual electrons in BeF as follows: in the $^2\Sigma$ state, $(2s\sigma)^2\,(3p\sigma)^2\,(2p\pi)^4\,(3s\sigma)$, and in the $^2\Pi_i$ state, $(2s\sigma)^2\,(3p\sigma)^2\,(2p\pi)^4\,(3p\pi)$. The assignment given for $^2\Sigma$ is identical with that for the $^2\Sigma$ state (normal state) of BO, CN and CO^+. For the $^2\Pi$ state, however, the arrangement differs from that proposed for the inverted $^2\Pi$ states of BO, etc., which are designated $(2s\sigma)^2\,(3p\sigma)^2\,(2p\pi)^3\,(3s\sigma)^2$, $^2\Pi$. This difference in interpretation is based on the fact that ΔE in the $^2\Pi$ state is much smaller for BeF than for the others ($\Delta E = 126$, 56, 126). No contradiction to Mulliken's conclusions is therefore contained in our assumption of a normal $^2\Pi$ state, with $\Delta E = 22.10$.

In conclusion, it is a pleasure to acknowledge several valuable suggestions in connection with this work from Professors R. T. Birge and R. S. Mulliken, as well as assistance in the measurements and computations from Mr. S. W. Nile and Professor F. W. Doermann.

---

[29] J. M. Walters and S. Barratt, Proc. Roy. Soc. **118A,** 120 (1928)

[30] R. S. Mulliken, Phys. Rev. **32,** 286 (1928).

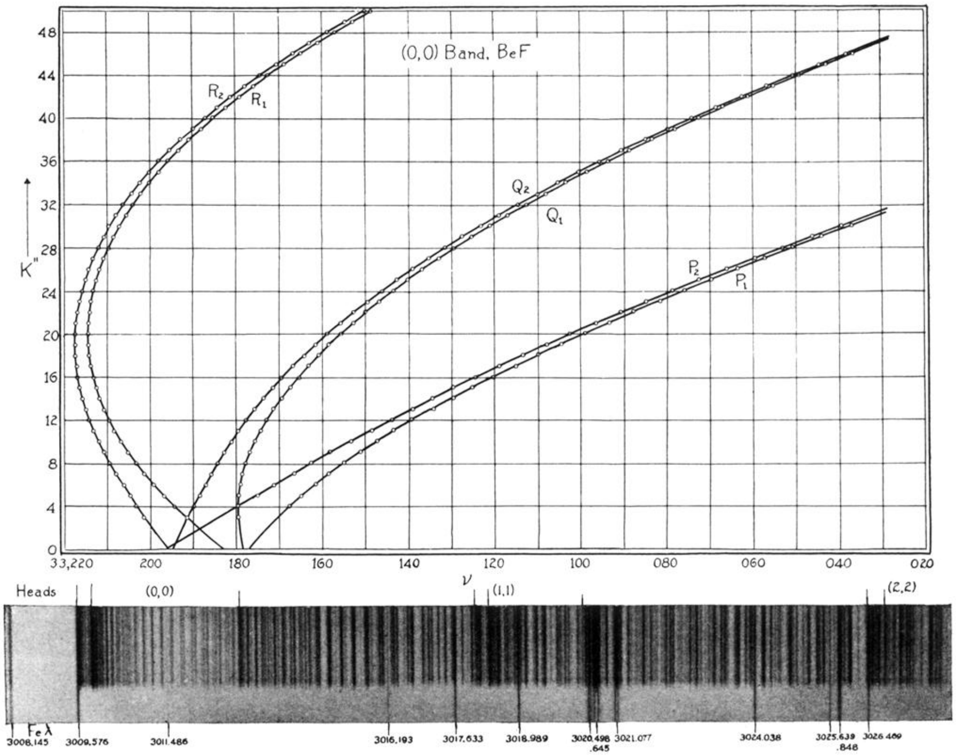

Fig. 1. (0, 0) *band of BeF.* The spectrum has been enlarged to practically the same scale as the diagram, but the correspondence of the lines with points on the diagram is not exact throughout, because the latter is on a scale of frequencies.